

Stokes and anti-Stokes double resonance Raman scattering in two-dimensional graphiteL. G. Cançado,¹ M. A. Pimenta,¹ R. Saito,² A. Jorio,¹ L. O. Ladeira,¹ A. Grueneis,² A. G. Souza-Filho,³ G. Dresselhaus,⁴ and M. S. Dresselhaus^{5,6}¹*Departamento de Física, Universidade Federal de Minas Gerais, Belo Horizonte, MG, 30123-970, Brazil*²*Department of Electronic-Engineering, University of Electro-Communications, Tokyo, 182-8585 Japan*³*Departamento de Física, Universidade Federal do Ceará, Fortaleza, CE, 60455-760, Brazil*⁴*Francis Bitter Magnet Laboratory, Massachusetts Institute of Technology, Cambridge, Massachusetts 02139-4307*⁵*Department of Physics, Massachusetts Institute of Technology, Cambridge, Massachusetts 02139-4307*⁶*Department of Electrical Engineering and Computer Science, Massachusetts Institute of Technology, Cambridge, Massachusetts 02139-4307*

(Received 27 February 2002; published 24 July 2002)

In this work, we discuss all possible double resonance processes which explain the observed features of the disorder-induced D band and its overtone, the G' -band, in Stokes (S) and anti-Stokes (AS) Raman spectra of two-dimensional graphite. It is shown that the D band is composed by two peaks, which are not associated with resonances with the incident and scattered photons, but rather are related to whether the first scattering of an electron is by a phonon or by a defect. The model explains the experimental results concerning the frequency shift of the D and G' bands in the S and AS spectra, as well as the fact that the G' band is not centered at two times the center of the D -band frequency.

DOI: 10.1103/PhysRevB.66.035415

PACS number(s): 78.30.Na, 78.66.Tr

I. INTRODUCTION

Graphitic materials exhibit a Raman band near 1350 cm^{-1} (the D band), which is activated by disorder or by the nanometric size of the graphite crystallites.¹ The D band has a dispersive behavior, since ω_D changes with the energy of the incident laser, the slope of the dispersion being about $50\text{ cm}^{-1}/\text{eV}$.²⁻⁵ Despite the fact that this band has been exhaustively studied in order to determine the crystallite size in graphitic materials, only recently has a double-resonance (DR) work has been proposed,⁶ which explains the special wave-vector selection of the phonon which gives rise to the dispersive D band in the Raman spectrum of graphite. However, this model does not explain the observed experimental shift of the D band in the Stokes (S) and anti-Stokes (AS) spectra, and the experimental fact that the frequency of the overtone G' band is not twice the D -band frequency. Saito *et al.*⁷ generalized the concept of the D -band double-resonance mechanism in graphite, and showed that it can be used to probe *all* phonon branches of graphite near the Γ and K points of the graphite 2D Brillouin zone.

In this work, we consider four possible DR mechanisms associated with scattering of electrons in either the S or AS process. The D band is therefore composed of two peaks D_1 and D_2 in the S spectra, and D_2 and D_3 in the AS spectra. On the other hand, the overtone of the D band, the G' band, is composed of a single peak, centered at $2\omega_{D_1}$ in the S spectrum and at $2\omega_{D_3}$ in the AS spectrum. Our model explains all observed features which were not understood previously, such as the shift of the D - and G' -band frequencies in the S and AS spectra, as well as the fact that the overtone G' band is not centered at twice the D -band frequency.

II. EXPERIMENTAL DETAILS

Stokes and anti-Stokes Raman scatterings were performed at room temperature, using a triple monochromator micro-

Raman spectrometer (DILOR XY) for the following laser energies: krypton 1.92 and 2.18 eV, and argon 2.41 and 2.54 eV. Stokes and anti-Stokes spectra were obtained under exactly the same conditions, in order to avoid any effect associated with different local temperatures and inhomogeneities in the sample. The laser power density used here was always less than $10^5\text{ W}/\text{cm}^2$.

The samples of two-dimensional (2D) graphite used in this work are low pressure chemical vapor deposition isotropic pyrolytic carbon and polyparaphenylene-based carbon, heat treated at 1500°C (PPP1500), both with crystallite sizes (L_a) around 50 \AA . The samples do not exhibit a stacking order along the c axis, and they can be considered as a good prototype of a 2D graphite.

III. RESULTS AND DISCUSSION

Figure 1 shows the S and AS Raman spectra of pyrolytic carbon in the D -band region, taken with laser incident energy of 2.41 eV. We can see that the D band is not centered at the same frequency in the S and AS spectra ($\omega_D^S \neq \omega_D^{AS}$); the D band in the S spectrum is downshifted by about 9 cm^{-1} compared to the corresponding band in the AS spectrum, and this result occurs for all laser energies used in this work. Despite the fact that the center of the D band depends on the laser intensity in both the S and AS spectra, we observed that the frequency difference ($\omega_D^{AS} - \omega_D^S$) does not change with laser power density. Figure 1 also shows the S and AS spectra of the overtone G' band. The horizontal scale for the G' -band spectra is on the upper axis of Fig. 1, which is twice the bottom axis, and was drawn in order to superimpose the first-order (D) and second-order (G') bands in the same figure measurements. Note that, in the S spectra, the center of the G' band is less than twice the frequency of the D band, whereas in the AS spectra, the G' -band frequency is more than twice the D -band frequency.

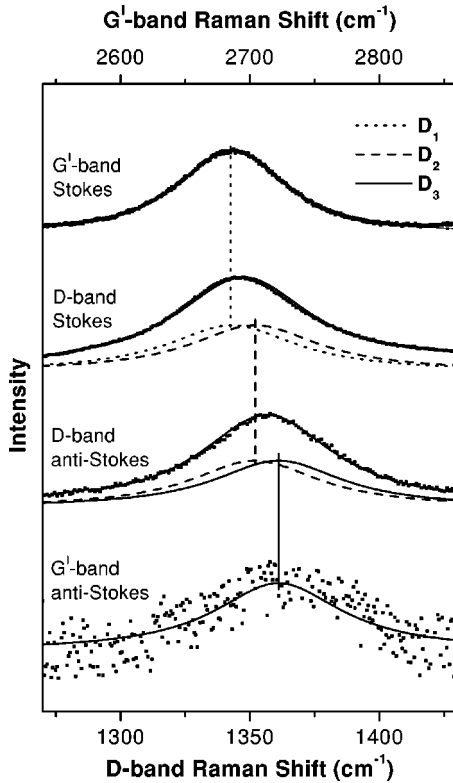


FIG. 1. Stokes and anti-Stokes Raman spectra of the D and G' bands in pyrolytic carbon obtained with $E_{\text{laser}} = 2.41$ eV, using a laser power density of 10^5 W/cm². The horizontal scale of the G' -band spectra was divided by two in order to compare these four bands in the same figure. The D band in the spectrum is fit by the peaks D_1 (dotted curve) and D_2 (dashed curve), and in the AS spectrum by the peaks D_2 (dashed curve) and D_3 (solid curve). The G' band in the S spectrum is fit by a single Lorentzian centered at $2\omega_{D_1}$, and in the AS spectrum by a Lorentzian centered at $2\omega_{D_3}$.

Our results concerning the frequencies of the D and G' bands are in agreement with several prior Raman studies of different types of sp^2 carbon materials, in which the G' -band frequency is always smaller than two times the D -band frequency in the Stokes spectra.^{2,4,8,9} The results presented in Fig. 1 are also in agreement with the Stokes and anti-Stokes study of graphite whiskers reported by Tan *et al.*,⁹ where the frequency difference for the G' band in the S and AS spectra (34 cm⁻¹) is about four times as large as the frequency difference of the D band (9 cm⁻¹).

As discussed below, a complete double resonance model is needed to fully explain the observed experimental S and AS results. We show here that the S and AS Raman D bands have a common peak which was not described previously.^{6,7} The D band is explained by an intervalley DR mechanism, involving transitions near two inequivalent K points at neighboring corners of the hexagonal first Brillouin zone of 2D graphite (K and K').⁷ The left part of Fig. 2 shows the four possible DR mechanisms associated with the D band in the Stokes process. For the first process, depicted in the upper part of Fig. 2 [process (a)], an electron with momentum $\hbar\mathbf{k}_0$ near the K point is resonantly excited from the π to the π^* band by an incident photon. In this case, the electron wave

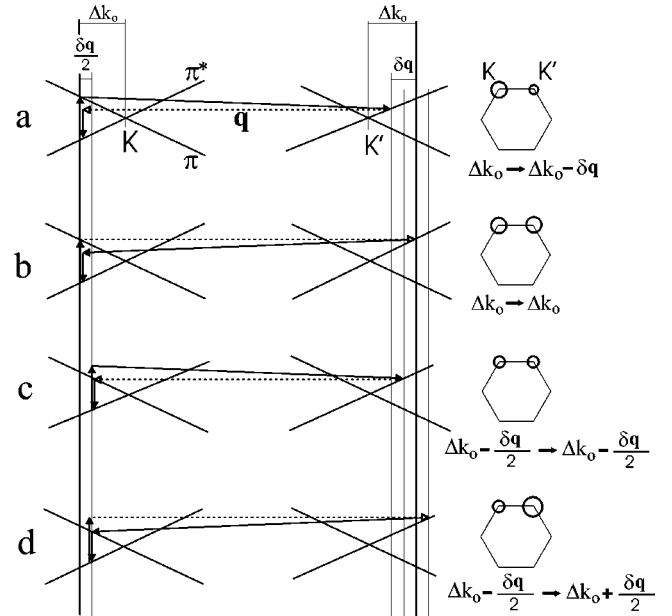


FIG. 2. The left side of the figure shows the four intervalley double-resonance processes for Stokes Raman scattering, with two points around the vertices K and K' of the Brillouin zone of graphite. The right side of the figure shows the circles around K and K' which correspond to the energy contours for the points that satisfy the DR mechanism, ignoring the trigonal warping effect. The radii of all circumferences are also shown in the figure.

vector has a distance $\Delta\mathbf{k}_0$ from the K point ($\Delta\mathbf{k}_0 = \mathbf{K} - \mathbf{k}_0$). The electron is then inelastically scattered, by the emission of a phonon with momentum $\hbar\mathbf{q}$, to a point near the K' point with momentum $\hbar(\mathbf{k}_0 + \mathbf{q})$ and energy $E(\mathbf{k}_0 + \mathbf{q})$ in the π^* band. This is a resonant process since it connects two real electronic states. The electron is scattered back to \mathbf{k}_0 by a defect or edge in a disordered graphite, and in this case the backscattering is elastic and non-resonant. Finally the electron-hole recombination process at \mathbf{k}_0 gives rise to a scattered photon with energy $E_{\text{laser}} - E_{\text{phonon}}$, which is not resonant with the $\pi^* - \pi$ transition.

In the second process depicted in Fig. 2 [process (b)], the scattering from a point around K to a point around K' is elastic and occurs *before* the inelastic backscattering, associated with the emission of the phonon. In processes (c) and (d) in Fig. 2, the incident photon is not in resonance with the $\pi - \pi^*$ transition, and the resonance occurs only for the scattered photon in the electron-hole recombination. In this case, the electron-hole pair must have a different momentum compared to processes (a) and (b). In process (c), the inelastic scattering of the electron occurs before the elastic backscattering, whereas in process (d) the elastic scattering occurs before the inelastic scattering process.

There are also four possible mechanisms associated with the anti-Stokes scattering, represented by processes (a), (b), (c), and (d) in Fig. 3, which are equivalent to the Stokes processes (a), (b), (c) and (d), in Fig. 2, respectively. The only difference in this case is that the inelastic scattering, connecting points around the K and K' points, is due to the *absorption* of a phonon with wave vector \mathbf{q} . Therefore, there

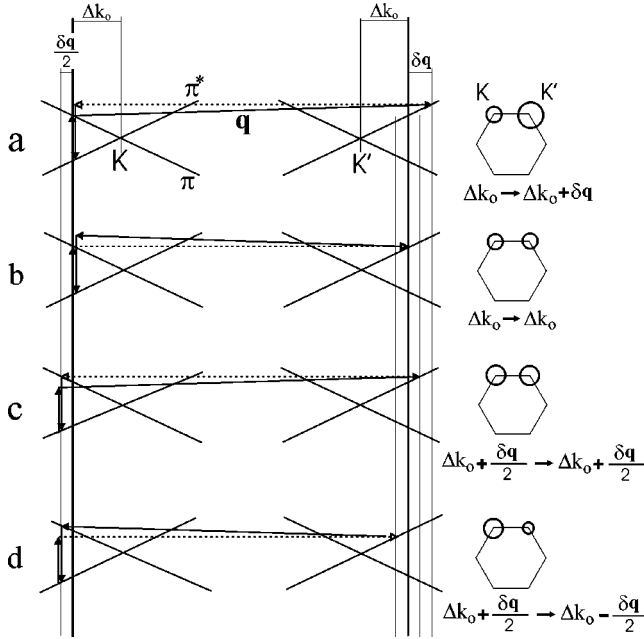


FIG. 3. The four intervalley double resonance processes for the anti-Stokes Raman scattering.

is an increase of $E_{\text{phonon}} = \hbar \omega_{\mathbf{q}}$ in the energy of the electron in the inelastic scattering process.

For points \mathbf{k} near the K point of graphite, the energy dispersion of the π electrons is symmetric around K and linearly proportional to $\Delta k = |\mathbf{K} - \mathbf{k}|$, that is,

$$E(\Delta k) = \pm A \Delta k, \quad (1)$$

where $A = \sqrt{3} \gamma_0 a / 2$, ($\gamma_0 = 2.90$ eV is the tight binding overlap integral parameter, and $a = 0.246$ nm is the graphite lattice parameter).¹⁰ The energy separation between these two bands is $\Delta E(\Delta k) = 2|E(\Delta k)|$. Therefore, for small Δk , the equienergy contour corresponds to circles around the K point. With increasing Δk , the energy contour changes continuously from a circle to a triangle, and this is known as the trigonal warping effect.¹¹ In the following analysis we will consider the equienergy contours around the K point given by points on the circumference of the circles, and the corrections introduced by the trigonal warping effect on the bandwidths will be discussed later in the paper.

The double-resonance processes associated with the D band connect points in the circles around K and K' , as shown in the right part of Figs. 2 and 3. Process (a) in Fig. 2 connects points on the circles around K and K' with radii Δk_0 and $\Delta k_0 - \delta q$, respectively, where δq is given by

$$\delta q = E_{\text{phonon}} / A. \quad (2)$$

Process (b) in Fig. 2 connects points along the two circles with the same radii Δk_0 around K and K' . In these two cases, the laser energy corresponds to the energy separation between the π and π^* bands, and therefore we have

$$E_{\text{laser}} = \Delta E(\Delta k_0) = 2A \Delta k_0. \quad (3)$$

TABLE I. Radii of the circles around the K and K' points, and the outer circle around K'' associated with all possible DR processes. The Raman peak associated with each process is also shown.

DR process	K circle	K' circle	K'' outer circle	Raman peak
S (a)	Δk_0	$\Delta k_0 - \delta q$	$2\Delta k_0 - \delta q$	D_1
S (b)	Δk_0	Δk_0	$2\Delta k_0$	D_2
S (c)	$\Delta k_0 - (\delta q)/2$	$\Delta k_0 - (\delta q)/2$	$2\Delta k_0 - \delta q$	D_1
S (d)	$\Delta k_0 - (\delta q)/2$	$\Delta k_0 + (\delta q)/2$	$2\Delta k_0$	D_2
AS (a)	Δk_0	$\Delta k_0 + \delta q$	$2\Delta k_0 + \delta q$	D_3
AS (b)	Δk_0	Δk_0	$2\Delta k_0$	D_2
AS (c)	$\Delta k_0 + (\delta q)/2$	$\Delta k_0 + (\delta q)/2$	$2\Delta k_0 + \delta q$	D_3
AS (d)	$\Delta k_0 + (\delta q)/2$	$\Delta k_0 - (\delta q)/2$	$2\Delta k_0$	D_2

For processes (c) and (d) in Fig. 2, the resonance occurs for the scattered photon, and in this case we have $\Delta E(\Delta k) = E_{\text{laser}} - E_{\text{phonon}}$. Therefore, using Eqs. (2) and (3) the radius of the circle around K is $\Delta k = \Delta k_0 - (\delta q)/2$. The circles around K' have radii $\Delta k_0 - (\delta q)/2$ and $\Delta k_0 + (\delta q)/2$ for processes (c) and (d), respectively.

Performing a similar analysis for the AS double resonance mechanism, we can determine the radii of the circles around K and K' associated with the four processes, and they are shown in the right part of Fig. 3. Table I shows the radii of the circles around K and K' for the four S and four AS double-resonance processes.

The double-resonance mechanism is satisfied by any phonon whose wave vector connects two points in the circles around K and K' , shown in the right part of Figs. 2 and 3. Figure 4 shows one of the possible DR mechanisms [process (a) in Fig. 2] where a phonon with wave vector \mathbf{q} connects two points along the circles with radii Δk_0 and $\Delta k_0 - \delta q$ around K and K' , respectively. If the vector \mathbf{q} is measured from the Γ (center) point in the Brillouin zone, its end is close to the K'' point in Fig. 4, which is equivalent to the K point by symmetry. As shown in Fig. 4, the set of all possible phonon \mathbf{q} vectors connecting any points in the circles around K and K' , measured from the Γ point, have ends in the area between the two circles around K'' . The radii of the inner and outer circle around K'' are respectively, δq and $2\Delta k_0 - \delta q$ and correspond to the modulus of the difference and the sum of the radii of the two circles around K and K' .

There is a high density of phonon wave vectors \mathbf{q} satisfying the DR mechanism for which the end of the wave vectors measured from the Γ point are in the inner and outer circles around K'' . The phonons associated with the singularities in the density of \mathbf{q} vectors are expected to make a significant contribution to the DR Raman spectra. Note that the radius of the inner circle around K'' ($\delta q = E_{\text{phonon}} / A$) does not depend on the laser energy. The associated DR phonon singularity gives rise to a weak band in the Raman spectra of disordered graphite around 1250 cm^{-1} , whose frequency does not depend on E_{laser} .⁷ A detailed calculation of the scattering matrix elements is needed in order to explain the in-

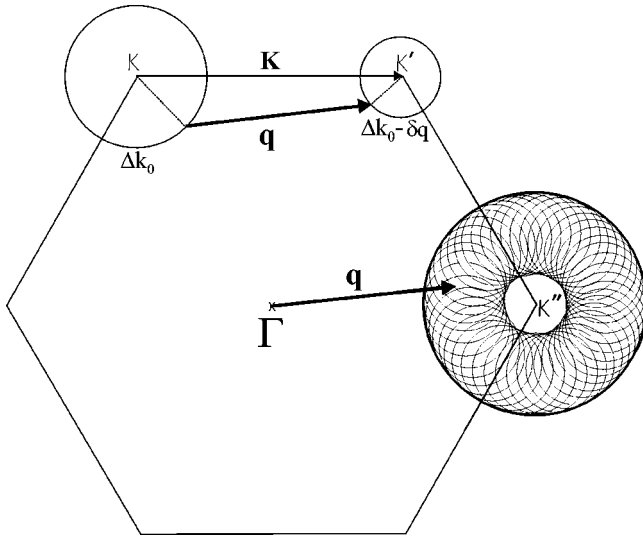


FIG. 4. One of the possible double-resonance (DR) Stokes Raman processes involving the emission of a phonon with wave vector \mathbf{q} . The set of all phonon wave vectors \mathbf{q} which are related to transitions from points on the two circles around K and K' gives rise to the collection of small circles around the K'' point. Note that this collection of circles is confined to a region between the two circles with radii δq and $2\Delta k_0 - \delta q$. The differences of the radii of the circles around K and K' and thus the radius of the inner circle around K'' were artificially enlarged for clarity.

tensity of the Raman peak around 1250 cm^{-1} . On the other hand, the D band is associated with the phonons with ends at the outer circle around K'' .

Table I also shows the radii of the outer circles around K'' . Note that these radii always involve the distance Δk_0 and thus, according to Eq. (3), they always depend on E_{laser} . The dependence of ω_D on the laser energy is explained by the E_{laser} dependence of the radius of the outer circle around K'' .⁷ According to the results presented in Table I, we must expect two peaks D_1 and D_2 in the S spectrum, associated with the two phonon singularities at $2\Delta k_0 - \delta q$ and at $2\Delta k_0$. For the AS spectrum, the corresponding two phonon singularities are at $2\Delta k_0$ and at $2\Delta k_0 + \delta q$, and the associated peaks are D_2 and D_3 , respectively. Moreover, the D_2 peak is expected to appear in both the S and AS spectra.

The double-resonance mechanism of the second-order G' band involves two phonons, instead of one phonon and one defect. In this case, only processes (a) and (c) in Figs. 2 and 3 are possible, since the resonant scattering from a circle around K to a circle around K' is always associated with the emission (or absorption) of a phonon. Therefore, we must expect a single peak for the G' band, centered at $2\omega_{D_1}$ and $2\omega_{D_3}$ in the Stokes and anti-Stokes spectra, respectively.

It is interesting to observe that, in the Stokes spectra, the D_1 peak is associated with processes (a) and (c) in Fig. 2, whereas D_2 is associated with processes (b) and (d) (see Table I). For the anti-Stokes mechanisms illustrated in Fig. 4, the highest frequency peak D_3 is associated with processes (a) and (c), whereas processes (b) and (d) give rise to the intermediate peak D_2 . Therefore, we conclude that the two peaks in the S and AS D band are not related to resonances

TABLE II. Frequencies and widths (in cm^{-1}) of the Lorentzians used to fit the D bands for different E_{laser} (in eV), measured using a low laser power density ($<10^5 \text{ W/cm}^2$). For a given E_{laser} , the widths of all peaks are the same.

E_{laser}	ω_{D_1}	ω_{D_2}	ω_{D_3}	γ_D
1.92	1324	1333	1342	64
2.18	1336	1345	1354	66
2.41	1352	1361	1370	69
2.54	1357	1366	1375	72

with the incident and scattered photons, but rather are associated with the scattering from a point around K to a point around K' , by a phonon [processes (a) and (c)] or by a defect [processes (b) and (d)].

Let us now estimate the frequency shift $\delta\omega_D$ between the two peaks which constitute the S and AS spectra. Considering that the phonon energy is much smaller than the visible photon energies ($E_{\text{phonon}} < E_{\text{laser}}/10$), we obtain $\Delta q \approx 2\Delta k_0$, where Δq is the distance of the phonon singularity from the K point ($\Delta q = |\mathbf{K} - \mathbf{q}|$). Therefore, using Eq. (3), the laser energy is given by $E_{\text{laser}} \approx A\Delta q$. Experimentally, it is known that the dispersion $\partial\omega_D/\partial E_{\text{laser}}$ is approximately $50 \text{ cm}^{-1}/\text{eV}$.⁵ We can thus write that $\partial\omega_D/\partial\Delta q = A \times 50 \text{ cm}^{-1}/\text{eV}$. The distance between the phonon singularities associated with the two peaks in both the S and AS spectra is $\delta q = E_{\text{phonon}}/A$, where E_{phonon} is approximately 0.17 eV . Therefore the shift between the two peaks which compose the D band is expected to be $\delta\omega_D = E_{\text{phonon}} \times 50 \text{ cm}^{-1}/\text{eV} = 8.5 \text{ cm}^{-1}$.

Figure 1 also shows the fit of the Stokes and anti-Stokes D and G' bands for $E_{\text{laser}} = 2.41 \text{ eV}$, according to the model discussed above. We adopted the following constraints in the fit procedure. The D band in the Stokes spectrum was fit by two Lorentzians centered at ω_{D_1} and ω_{D_2} , and in the anti-Stokes spectrum by two Lorentzians at ω_{D_2} and ω_{D_3} . We kept the same width and intensity for the three Lorentzians, for a given laser energy, and the D_2 frequency was always the same in the S and AS spectra. On the other hand, the G' band was fit by a single Lorentzian, centered at $2\omega_{D_1}$ in the S spectrum and at $2\omega_{D_3}$ in the AS spectrum. Table II shows the fitting parameters of the Stokes and anti-Stokes Raman D band of PPP1500, for incident laser energies $E_{\text{laser}} = 1.92, 2.18, 2.41, \text{ and } 2.54 \text{ eV}$, respectively, measured using a low laser power density ($<10^5 \text{ W/cm}^2$). The errors in the frequencies and widths (full widths at half maximum) of the Lorentzians are about 2 and 4 cm^{-1} , respectively.

It is interesting to note that the experimental shift of the D band in the S and AS spectra, of about 9 cm^{-1} , is related to the mean frequencies $(\omega_{D_1} + \omega_{D_2})/2$ and $(\omega_{D_2} + \omega_{D_3})/2$ of the S and AS D bands, which is in excellent agreement with the theoretical value of 8.5 cm^{-1} . On the other hand, the shift of the G' band in the S and AS spectra is expected to be $2(\omega_{D_3} - \omega_{D_1}) = 34 \text{ cm}^{-1}$, which is also in excellent agreement with the results shown in Fig. 1 and the results reported in Ref. 9.

It can be observed in Fig. 1 that the two Stokes (or the two anti-Stokes) peaks cannot be resolved in the experimental Raman D band, since their widths are much larger than the frequency separation $\delta\omega_D$. An important contribution to the linewidth is the trigonal warping effect, since the energy contour of the electron dispersion is modified from a circle to a triangle with increasing Δk_0 .¹¹ Therefore, the distribution of wave vectors δk_0 associated with a given energy separation between the π and π^* bands increases with increasing Δk_0 . Note in Table II that the widths of the Lorentzians increase slightly with increasing E_{laser} . This is a clear manifestation of the trigonal warping effect, which is more important for higher laser energies.¹¹

IV. CONCLUSION

In summary, we have presented a complete model which explains all observed features in the S and AS spectra of 2D graphitic materials that were not understood previously, that is, the experimental frequency shift of the D and G' bands in the S and AS spectra, and the fact that the G' band is not centered at two times the D -band frequency. The D band in the S spectrum is composed of two peaks with frequencies ω_{D_1} and ω_{D_2} , and the overtone G' band is composed of a

single peak centered at $2\times\omega_{D_1}$. For the anti-Stokes spectra, the D band is also composed of two peaks centered at ω_{D_2} and ω_{D_3} , and the G' band is centered at $2\times\omega_{D_3}$. The experimental results for the D and G' bands in the S and AS spectra of different sp^2 carbon materials are in excellent agreement with the model. It is also shown that the splitting of the D band into two peaks is not associated with resonances with the incident and scattered photons, but rather is related to whether the first scattering event is by a phonon or by a defect.

ACKNOWLEDGMENTS

We thank Professor M. Endo for providing us with the PPP-1500 sample. We gratefully acknowledge the NSF/CNPq joint collaboration program (NSF Grant No. INT. 00-00408 and CNPq Grant No. 910120/99-4). The MIT authors acknowledge support under NSF Grant No. DMR 01-16042. R.S. acknowledges UFMG for supporting the visit to UFMG and a Grant-in-Aid (No. 13440091) from the Ministry of Education and Science, Japan. L.G.C., A.J. and A.G.S.F. acknowledge support from the Brazilian Agencies CAPES and CNPq.

¹F. Tuinstra and J. L. Koenig, J. Chem. Phys. **53**, 1126 (1970).

²R. P. Vidano, D. B. Fishbach, L. J. Willis, and T. M. Loehr, Solid State Commun. **39**, 341 (1981).

³A. V. Baranov, A. N. Bekhterev, Y. S. Bobovich, and V. I. Petrov, Opt. Spektrosk. **62**, 1036 (1987) [Opt. Spectrosc. **62**, 612 (1987)].

⁴Y. Wang, D. C. Alsmeyer, and R. L. McCreery, Chem. Mater. **2**, 557 (1990).

⁵M. J. Matthews, M. A. Pimenta, G. Dresselhaus, M. S. Dresselhaus, and M. Endo, Phys. Rev. B **59**, R6585 (1999).

⁶C. Thomsen and S. Reich Phys. Rev. Lett. **85**, 5214 (2000).

⁷R. Saito, A. Jorio, A. G. Souza Filho, G. Dresselhaus, M. S.

Dresselhaus, and M. A. Pimenta, Phys. Rev. Lett. **88**, 027401 (2002).

⁸P. H. Tan, Y. M. Deng, and Q. Zhao, Phys. Rev. B **58**, 5435 (1998).

⁹P. H. Tan, C. Y. Hu, J. Dong, W. C. Shen, and B. F. Zhang, Phys. Rev. B **64**, 214301 (2001).

¹⁰R. Saito, G. Dresselhaus, and M. S. Dresselhaus, *Physical Properties of Carbon Nanotubes* (Imperial College Press, London, 1998).

¹¹R. Saito, G. Dresselhaus, and M. S. Dresselhaus, Phys. Rev. B **61**, 2981 (2000).